



**CHALMERS**  
UNIVERSITY OF TECHNOLOGY

## **Characterization of two $\beta$ -galactosidases LacZ and WspA1 from *Nostoc flagelliforme* with focus on the latter's central active region**

Downloaded from: <https://research.chalmers.se>, 2023-05-05 08:40 UTC

Citation for the original published paper (version of record):

Gao, X., Liu, L., Cui, L. et al (2021). Characterization of two  $\beta$ -galactosidases LacZ and WspA1 from *Nostoc flagelliforme* with focus on the latter's central active region. *Scientific Reports*, 11(1).  
<http://dx.doi.org/10.1038/s41598-021-97929-6>

N.B. When citing this work, cite the original published paper.



OPEN

# Characterization of two $\beta$ -galactosidases LacZ and WspA1 from *Nostoc flagelliforme* with focus on the latter's central active region

Xiang Gao<sup>1,2✉</sup>, Litao Liu<sup>2</sup>, Lijuan Cui<sup>2</sup>, Tao Zheng<sup>1</sup>, Boyang Ji<sup>3</sup> & Ke Liu<sup>2</sup>

The identification and characterization of new  $\beta$ -galactosidases will provide diverse candidate enzymes for use in food processing industry. In this study, two  $\beta$ -galactosidases, Nf-LacZ and WspA1, from the terrestrial cyanobacterium *Nostoc flagelliforme* were heterologously expressed in *Escherichia coli*, followed by purification and biochemical characterization. Nf-LacZ was characterized to have an optimum activity at 40 °C and pH 6.5, different from that (45 °C and pH 8.0) of WspA1. Two enzymes had a similar Michaelis constant ( $K_m = 0.5$  mmol/liter) against the substrate o-nitrophenyl- $\beta$ -D-galactopyranoside. Their activities could be inhibited by galactostatin bisulfite, with IC50 values of 0.59  $\mu$ M for Nf-LacZ and 1.18  $\mu$ M for WspA1, respectively. Gel filtration analysis suggested that the active form of WspA1 was a dimer, while Nf-LacZ was functional as a larger multimer. WspA1 was further characterized by the truncation test, and its minimum central region was found to be from residues 188 to 301, having both the glycosyl hydrolytic and transgalactosylation activities. Finally, transgenic analysis with the GFP reporter protein found that the N-terminus of WspA1 (35 aa) might play a special role in the export of WspA1 from cells. In summary, this study characterized two cyanobacterial  $\beta$ -galactosidases for potential applications in food industry.

$\beta$ -galactosidase (EC 3.2.1.23), commonly known as lactase, is one of the most important enzymes used in food processing industry<sup>1,2</sup>. This enzyme catalyzes the hydrolysis of  $\beta$ -galactosides from polymers, oligosaccharides or secondary metabolites by breaking the  $\beta$ -D-galactosidic linkages<sup>3</sup>. In addition to the hydrolytic activity, some  $\beta$ -galactosidases also possess the transgalactosylation activity, which involves the process of transferring galactose to another carbohydrate instead of water<sup>4</sup>. Thus, this enzyme has two main applications including the removal of lactose from milk products and the production of galactosylated products such as galacto-oligosaccharides (GOS). The lactose-hydrolyzed milk products can meet the need of lactose-intolerant people, while GOS is one of the important human prebiotics<sup>5</sup>.

$\beta$ -galactosidases are distributed in a variety of sources including bacteria, fungi, and plants<sup>1,6</sup>. They are categorized into the glycoside hydrolase (GH) families GH1, GH2, GH35, GH42, GH59, and GH147 based on their similarities<sup>2</sup>.  $\beta$ -galactosidases from these GH families belong to the superfamily Clan-A and share the ( $\alpha/\beta$ )8 barrel structure<sup>7</sup>. The well-known *Escherichia coli*  $\beta$ -galactosidase LacZ belongs to the GH2 family and has been structurally elucidated<sup>8,9</sup>. The functionally active form of *E. coli* LacZ is a homotetramer with each monomer comprising of five structural domains, and the third (central) domain (residues 334–627) is an ( $\alpha/\beta$ )8 barrel with an extended active-site cleft. Different sources of  $\beta$ -galactosidases differ in their optimum pH and temperature, thermal stability, substrate specificity, and metal ion cofactor sensitivity, providing a diversified selection for application in food processing<sup>1,2,10–12</sup>. Therefore, identification and characterization of new  $\beta$ -galactosidases from natural resources is beneficial for establishing glycosidase libraries and offers a wide variety of candidate glycosidases for application in food industry. Photosynthetic microorganisms (microalgae and cyanobacteria) serve as

<sup>1</sup>School of Food and Biological Engineering, Shaanxi University of Science and Technology, Xi'an 710021, China. <sup>2</sup>School of Life Sciences, Central China Normal University, Wuhan 430079, China. <sup>3</sup>Department of Biology and Biological Engineering, Chalmers University of Technology, 41296 Gothenburg, Sweden. ✉email: xianggao@sust.edu.cn

Primer no., name	Primer sequence (5'-3')	Primer combination
1, Nf-LacZ-F	ggaattcCATATGAAATTGTTGGATATACA	/
2, Nf-LacZ-R	cgGGATCCTTAACAGCTTGTGGGAGTACAT	1 + 2, for Nf-LacZ
3, Wsp <sub>A</sub> -F	ggaattcCATATGGTAGATCAGCCTTTTGTCTCC	/
4, Wsp <sub>A</sub> -R	cgGGATCCTTATTTCATTACAAATGCAAAG	3 + 4, for Wsp <sub>A</sub>
5, Wsp <sub>C1</sub> -F	ggaattcCATATGACTACAGCTAATCCTGGAAC	/
6, Wsp <sub>C1</sub> -1R	cgGGATCCTTAACCTAAACCTAGACCTGATG	5 + 6, for Wsp <sub>C1</sub>
7, Wsp <sub>C2</sub> -2R	cgGGATCCTTAACAGTTTCCAGCCAACCGA	5 + 7, for Wsp <sub>C2</sub>
8, Wsp <sub>C3</sub> -3R	cgGGATCCTTAATCTGCGTTGACATTCAAAG	5 + 8, for Wsp <sub>C3</sub>
9, Wsp <sub>C4</sub> -4R	cgGGATCCTTACTCACCAGTGAGCAGATCGA	5 + 9, for Wsp <sub>C4</sub>
10, WspA1-F	ATGTCGTTAAAGACTTTTAG	/
11, WspA1-R	TTCATTACAAATGCAAAG	10 + 11, for WspA1::GFP
12, Wsp <sub>B</sub> -F	ATGGCTCTTTACGGCTATAC	12 + 11, for Wsp <sub>B</sub> ::GFP
13, Wsp <sub>N</sub> -R	cccCTCGAGAATTTCTCCTTATTGAA	10 + 13, for Wsp <sub>N</sub> ::GFP

**Table 1.** The PCR primers used in this study. The protective bases in the primers were shown in lowercase letters.

promising resources to excavate the intra- and extra-cellular  $\beta$ -galactosidases<sup>13–15</sup>. However, the reports about the biochemical characterization of new  $\beta$ -galactosidases from microalgae or cyanobacteria are still relatively few.

*Nostoc flagelliforme* is a soil surface-dwelling cyanobacterium inhabiting the xeric steppes of western China<sup>16</sup>. It exhibits a predominantly filamentous (hair-like or cylindrical) colony shape. In previous studies, an acidic water stress protein, WspA, was identified to be a novel  $\beta$ -galactosidase in *N. flagelliforme* and its close relative *Nostoc commune*<sup>17,18</sup>. WspA was synthesized in cells under ultraviolet irradiation or desiccation stress and secreted into extracellular polysaccharide matrix upon rehydration<sup>19</sup>. It was recently reported that *wspA* sequences showed high polymorphism in *N. flagelliforme* colonies<sup>20</sup>. In the sequenced *N. flagelliforme* CCNUN1 (NCBI BioProject, PRJNA407846), there are two adjacent *wspA* genes (COO91\_01770 and COO91\_01773)<sup>21</sup>. In the sequenced *N. commune* HK-02 and *Nostoc sphaeroides* CCNUC1, there is one (NIES4070\_53480) and three (GXM\_06477, GXM\_06476, and GXM\_06474) *wspA* genes, respectively. *wspA1* gene was first reported in *N. commune*<sup>19</sup> and was also amplified by PCR in *N. flagelliforme* colonies<sup>18</sup>. Since the recombinant full-length WspA1 was always expressed as inclusion bodies in *E. coli* protein expression system, we had generated two truncated proteins of WspA1 (Wsp<sub>A</sub> and Wsp<sub>B</sub>) for biochemical characterization<sup>18</sup>. The effects of temperature, pH, and metal ions on the activities of Wsp<sub>A</sub> and Wsp<sub>B</sub> as well as their catalytic constant *K<sub>m</sub>* were characterized in our previous study. The enzymatic activity of Wsp<sub>A</sub> was stronger than that of Wsp<sub>B</sub>. However, there still remain some uncharacterized biochemical features for WspA1, such as the active form (monomer or multimer), enzymatic inhibitors, the active center, and so on. In addition, the potential homologs of the well-known  $\beta$ -galactosidase LacZ in *N. flagelliforme* have also not been characterized so far. In the present study, we identified a LacZ in *N. flagelliforme* (hereinafter Nf-LacZ) and conducted comparative biochemical analysis of Nf-LacZ and WspA1. Further, we focused on WspA1 to explore its central active region by using the protein truncation test. Besides, we investigated the possible role of the specific N-terminus of WspA1.

## Material and methods

**Cloning of  $\beta$ -galactosidase genes in *N. flagelliforme*.** The potential  $\beta$ -galactosidase LacZ in *N. flagelliforme* was identified by local blasting (BioEdit software) against the proteome fasta file of *N. flagelliforme* CCNUN1 with the well-known *E. coli* (strain K12) LacZ (JW0335, KEGG)<sup>9</sup>. The resulting LacZ homolog is AUB41471 (NCBI), which is encoded by the gene COO91\_07519 (KEGG). Nf-LacZ sequence was amplified by PCR from genomic DNA of the *N. flagelliforme* culture in our laboratory. The NCBI accession no. for WspA1 is ABA54841 and its complete CDS can be retrieved from NCBI accession no. DQ155425. Various truncated sequences of *wspA1* were amplified by PCR from our previously constructed plasmid pMD18-T::*wspA1*<sup>22</sup>. The PCR primers used in this part (primer no. 1–9) were summarized in Table 1. PCR products were digested with the restriction endonucleases *Nde* I and *Bam*HI and constructed into the plasmid pET28a between the same restrictive sites. All the constructions were verified by sanger sequencing.

**In vitro expression and purification.** The *E. coli* BL21(DE3)/pET28a protein expression system (Novagen, USA) was used to express target proteins. The above constructs were transformed into the *E. coli* strain to produce target proteins with His-tags at the N-terminus. The transformed *E. coli* strains were grown in 200 mL LB medium (containing 50  $\mu$ g/mL kanamycin) at 37 °C and 220 rpm until the optimum density at 600 nm (OD<sub>600</sub>) reached up to 0.5–0.6, and then the cultures were subjected to protein induction for 6 h with 0.2 mM Isopropyl  $\beta$ -D-thiogalactoside (IPTG). After centrifugation, the pellets were crushed by a low-temperature high-pressure crusher. The crude proteins were loaded on Ni His•Bind resin gravity column (Novagen, USA). The column was washed with the buffer (20 mM Tris-HCl, 500 mM NaCl, 80 mM imidazole, 5% glycerol, pH 8.0) to remove unwanted proteins and then the target protein was eluted with the buffer (20 mM Tris-HCl, 500 mM NaCl, 1000 mM imidazole, 5% glycerol, pH 8.0). Protein profiling or separation was examined using 12% sodium dodecyl sulfate–polyacrylamide gel electrophoresis (SDS-PAGE)<sup>23</sup>. If necessary, eluted proteins

were further purified by gel filtration with fast protein liquid chromatography (FPLC) system (AKTA purifier, GE Healthcare, Sweden), which was equipped with an anion exchange column HiTrap Q FF (16 × 25 mm, GE Healthcare)<sup>24</sup>. Protein concentration was determined with the Bradford assay<sup>25</sup>.

**Protein polymerization assay.** The gel filtration with the FPLC system can be also employed to analyze the polymerization state of native or active proteins<sup>26</sup>. Protein samples were injected into the column for separation, which was equilibrated with the buffer (20 mM Tris-HCl, 150 mM NaCl, 10% glycerol, pH 7.5). Five molecular weight markers were used: beta-amylase (200 kDa), alcohol dehydrogenase (150 kDa), albumin (66 kDa), carbonic anhydrase (29 kDa), and cytochrome c (12.4 kDa) (GE Healthcare, China agency). Protein separation was monitored by measuring the absorbance at 280 nm. To analyze the effects of acidic or more alkaline conditions on the protein polymerization state, the above-mentioned buffer was adjusted to pH 5.5 and 8.5, respectively.

**Galactosidase activity assay.** Galactosyl hydrolytic and transgalactosylation activities of the target proteins were assayed as previously described<sup>18</sup> with slight modifications. Galactosyl hydrolytic activity was assayed in 1 ml of 0.1 M phosphate-buffered saline (PBS) solution (pH 7.5) with 3 mM o-nitrophenyl-β-D-galactopyranoside (ONPG) as the substrate. The final protein concentration used for the reaction was 10 µg/ml. The reactions were conducted at 37 °C and stopped by supplementation with 100 µl of 1 M Na<sub>2</sub>CO<sub>3</sub> solution. The absorbance of the reaction product o-nitrophenol (ONP) was measured at 405 nm.

Transgalactosylation reactions were performed at 37 °C for 3 h by incubation of 20 µg/ml enzyme (final concentration) with 20 µl of the acceptor glucose (500 mM) and 60 µl of ONPG (50 mM) in 100 µl of 0.1 M PBS buffer (pH 7.5). Products of the transgalactosylation reaction were examined by thin-layer chromatography (TLC)<sup>27</sup>. Each reaction solution of 2 µl was dropped on the silica gel plate for TLC analysis with methanol:chloroform (40:60) as the mobile phase. After the chromatography, the plate was air-dried at room temperature. The chromatogram observation was performed by spraying 20% H<sub>2</sub>SO<sub>4</sub> on the silica gel plate and heating at 115 °C for 15 min.

**Enzymatic inhibitor assay.** Enzymatic inhibition reaction was conducted in the above-mentioned galactosyl hydrolytic solution by supplementing various concentrations of glycosidase inhibitors. Four inhibitors were used: 4-methylumbelliferyl-beta-D-glucopyranoside (4-MU-Glu), conduritol B epoxide (CBE), acarbose, and galactostatin bisulfite (GBS) (ALFA Chemistry, USA). The reaction was conducted at 37 °C. The protein concentration was 10 µg/ml. Similarly, the absorbance at 405 nm of the reaction product was measured. For evaluating the inhibitory effects of these inhibitors, the concentration range of 0 ~ 200 µM and the extended reaction time of 9 h were considered in the initial test.

The half-maximal inhibitory concentration (IC<sub>50</sub>) represents the concentration of a substance (e.g. a drug) that is required for 50% inhibition in a specific biological or biochemical function<sup>28</sup>. The IC<sub>50</sub> values of the galactosidases in response to GBS inhibition were assayed as previously described<sup>29</sup> with slight modification. For IC<sub>50</sub> detection, the reaction was conducted at 37 °C for 3 h, with the concentrations of GBS ranging from 0 to 50 µM.

**Expression of GFP-fused proteins in *Nostoc* sp. PCC 7120.** Three nucleotide sequences, *wspA1*, the N-terminal sequence of *wspA1* (*wsp<sub>N</sub>*), and the truncated sequence of *wspA1* without *wsp<sub>N</sub>* (*wsp<sub>B</sub>*), were amplified by PCR from the plasmid pMD18-T::wspA1 with the primers (primer no. 10–13) as shown in Table 1. For generating green fluorescent protein (GFP) gene-fused constructions, a plasmid pRL25C-GFP<sup>30</sup> was modified by introducing a *petE* promoter<sup>31</sup> and two adjacent restriction sites *Sma* I and *Xho* I, and then the PCR products were inserted into the modified plasmid. Plasmid transformation and transformant selection were performed as previously described<sup>32</sup>. GFP fluorescence signals in the transgenic cells were observed by confocal laser-scanning microscopy (Leica, Germany). GFP was excited at 488 nm by an argon-ion laser.

**Western blotting analysis.** The above transgenic cells at the exponential period (OD<sub>750</sub> of 0.4 ~ 0.6) were collected by centrifugation at 6,000 rpm for 5 min. The pelleted cells were subjected to protein extraction and the crude protein extracts were separated on 12% SDS-PAGE gels for western blotting as previously described<sup>22</sup>. Anti-WspA1 rabbit antiserum was used for the blotting. In addition, the remaining supernatants were filtered with double filter papers to remove residual cells. The initial chlorophyll fluorescence (*F<sub>0</sub>*) of possibly residual cells in the filtered solutions was detected by a plant efficiency analyzer (Hansatech Instruments Ltd., UK)<sup>33</sup>. The *F<sub>0</sub>* value of zero confirmed no cell contamination. The solutions were freeze-dried and the pellets (containing the released proteins) were subjected to western blotting as the above-mentioned.

**Phylogenetic analysis.** The Nf-LacZ sequence was used to query the KEGG database with BLAST, and the resulting top 50 hits were retrieved from the database. The LacZ from *E. coli* MS 85–1 (b0344, KEGG) was used as an outgroup. The amino acid sequences were aligned using mafft<sup>34</sup>. The resulting sequence alignments were adjusted using trimAl<sup>35</sup> by removing spurious sequences. The maximum-likelihood phylogenetic tree was inferred using IQ-Tree 2.1.2<sup>36</sup> with the LG + F + R5 model and 1,000 bootstraps.

## Results

**Identification of the β-galactosidase LacZ in *N. flagelliforme*.** The potential homologs of the β-galactosidase LacZ have not yet been identified in *N. flagelliforme*. In this study, a putative Nf-LacZ (COO91\_07519) was identified as described in the methods. Nf-LacZ consists of 619 amino acid residues with a

calculated molecular weight of 70.8 kDa. The Pfam domain analysis showed that Nf-LacZ possesses the TIM barrel domain and the sugar-binding domain of GH family 2. Phylogenetic analysis suggested that LacZ homologs from cyanobacterial species form a distinct clade (Fig. 1).

The recombinant Nf-LacZ was expressed by employing the *E. coli* expression system. As shown in the SDS-PAGE gel, Nf-LacZ was effectively induced and then separated (Fig. 2A). Gel filtration with FPLC is often used to analyze or purify mixtures of proteins according to size and charge<sup>37</sup>. Based on the molecular weight markers in this FPLC analysis (Fig. 2B), native Nf-LacZ should be a multimeric protein (at least a trimer or larger). The effects of pH and temperature on the enzymatic activity were also assayed using ONPG as a substrate. The optimum temperature and pH for Nf-LacZ are 40 °C and pH 6.5, respectively (Supplemental Fig. S1). Metal ions may also affect the activity of the  $\beta$ -galactosidase. It was found that the metal ions,  $K^+$ ,  $Mg^{2+}$ ,  $Ca^{2+}$ ,  $Zn^{2+}$ , and  $Mn^{2+}$  can all enhance the enzymatic activity of Nf-LacZ (Supplemental Fig. S1). In contrast, the optimum temperature and pH for Wsp<sub>A</sub> are 45 °C and pH 8.0, respectively, and  $Ca^{2+}$  and  $Zn^{2+}$  are inhibitory for the activity of Wsp<sub>A</sub><sup>18</sup>. Further, the kinetic parameters  $K_m$  and  $V_{max}$  of Nf-LacZ were determined with ONPG as the substrate (Fig. 2C). The  $K_m$  value was 0.5 mmol/liter for Nf-LacZ, which is close to that of Wsp<sub>A</sub><sup>18</sup>. Thus, Nf-LacZ has a similar affinity as Wsp<sub>A</sub> for ONPG under the tested condition.

**Analysis of the polymerization of native Wsp<sub>A</sub>.** Wsp<sub>A</sub> consists of 234 amino acid residues with a calculated molecular weight of 24.0 kD. The polymerization state of native Wsp<sub>A</sub> was not explored in our previous study. As shown in the SDS-PAGE gel, the recombinant Wsp<sub>A</sub> that was expressed by the *E. coli* expression system was separated (Fig. 3A). Subsequently, the polymerization state of native Wsp<sub>A</sub> was analyzed by FPLC (Fig. 3B). FPLC fraction of Wsp<sub>A</sub> was between the 29 and 66 kDa makers, implying that native Wsp<sub>A</sub> is not a monomer but a dimer. Our previous study showed that Wsp<sub>A</sub> had a narrow optimal pH range; at pH 5.5, the activity of Wsp<sub>A</sub> reduced to nearly zero, while at pH 8.5 the activity decreased more than 60% compared to the maximum activity at pH 8.0<sup>18</sup>. However, FPLC analysis showed that the dimer of Wsp<sub>A</sub> was not dissociated at both pH 5.5 (Fig. 3C) and pH 8.5 (Fig. 3D). Therefore, native Wsp<sub>A</sub> forms a stable dimer although its activity can be affected by the unfavorable acid–base environment.

**Effects of the inhibitors on the activities of Nf-LacZ and Wsp<sub>A</sub>.** The response of the glycosidase to various inhibitors is an important aspect for characterization. The influences of glycosidase inhibitors on the activities of Nf-LacZ and Wsp<sub>A</sub> were investigated. Totally four inhibitors, 4-MU-Glu, CBE, acarbose, and GBS, were used for testing. Among them, 4-MU-Glu, CBE, and acarbose did not show obvious inhibitory effects on both enzymes. The inhibitory effects of GBS on the two enzymes were then compared (Fig. 4). The activities of both Nf-LacZ (Fig. 4A) and Wsp<sub>A</sub> (Fig. 4B) were markedly inhibited by 0.1  $\mu$ M GBS. The IC<sub>50</sub> value is widely used as the informative measure of an enzyme inhibitor's efficacy<sup>28</sup>. The results showed that Nf-LacZ had an IC<sub>50</sub> value of 0.59  $\mu$ M (Fig. 4C), while Wsp<sub>A</sub> had a IC<sub>50</sub> value of 1.18  $\mu$ M (Fig. 4D). Thus, Wsp<sub>A</sub> was relatively less sensitive to the inhibitor GBS at the tested condition.

**Identification of the central activity region of WspA1.** The recombinant WspA1 was always expressed as inclusion bodies in *E. coli* cell and thus expression of its truncated proteins was one way to explore its biochemical functions<sup>18</sup>. To investigate the central activity region of WspA1, we designed four truncated WspA1 variants (Wsp<sub>C1</sub>, Wsp<sub>C2</sub>, Wsp<sub>C3</sub>, and Wsp<sub>C4</sub>) in this study (Fig. 5A), roughly according to its secondary structure predicted by PSIPRED<sup>38</sup>. The four truncated proteins were in vitro expressed and purified (Fig. 5B). Their catalytic features as a  $\beta$ -galactosidase were assayed using ONPG and 5-bromo-4-chloro-3-indolyl- $\beta$ -D-galactoside (X-Gal) as the substrates. The biochemical analysis showed that Wsp<sub>C1</sub>, Wsp<sub>C2</sub>, and Wsp<sub>C3</sub> had a successively decreased galactosyl hydrolytic activity, while Wsp<sub>C4</sub> did not show the activity (Fig. 5C,D). Further, the potential transgalactosylation activities of Wsp<sub>C1</sub>, Wsp<sub>C2</sub>, and Wsp<sub>C3</sub> were assayed by TLC with glucose as the acceptor (Fig. 5E). The result showed that the disaccharide or oligosaccharide was produced under the catalysis of Wsp<sub>C1</sub> and Wsp<sub>C2</sub>, while Wsp<sub>C3</sub> had no this catalytic activity. Therefore, Wsp<sub>C2</sub> should represent the minimum active region of WspA1 with both hydrolytic and transgalactosylation activities up to now.

**Analysis of the role of the N-terminus of WspA1 in secretion.** As implied in our previous attempts, the N-terminus of WspA1 (Wsp<sub>N</sub>) was a potential cause for the forming of inclusion bodies in the *E. coli* expression system. We further speculated that Wsp<sub>N</sub> might have a potential role in facilitating the export of WspA1 from cells, since Wsp<sub>A</sub> can be secreted into extracellular polysaccharide matrix upon rehydration<sup>19</sup>. WspA1, Wsp<sub>B</sub> (the WspA1 protein lacking Wsp<sub>N</sub>), and Wsp<sub>N</sub> were respectively fused with the GFP protein, and their features regarding extracellular transport were examined in transgenic cells by confocal microscopy (Fig. 6A–C). In WspA1::GFP cells, sporadic fluorescent foci were observed in the periplasmic space (Fig. 6A), while no such fluorescent foci were observed in Wsp<sub>B</sub>::GFP cells (Fig. 6B). In Wsp<sub>N</sub>::GFP cells, fluorescent foci were scattered in cells and some of them seemed to be in the process of secretion (Fig. 6C). In addition, the crude proteins that were extracted from WspA1::GFP and Wsp<sub>B</sub>::GFP cells and their culture solutions were subjected to western blotting using anti-WspA1 antibody (Fig. 6D). WspA1 was detected in both its transgenic cells and the culture solution, while Wsp<sub>B</sub> was only detected in its transgenic cells. Together, these results implied that Wsp<sub>N</sub> had a potential role in facilitating the secretion of WspA1.



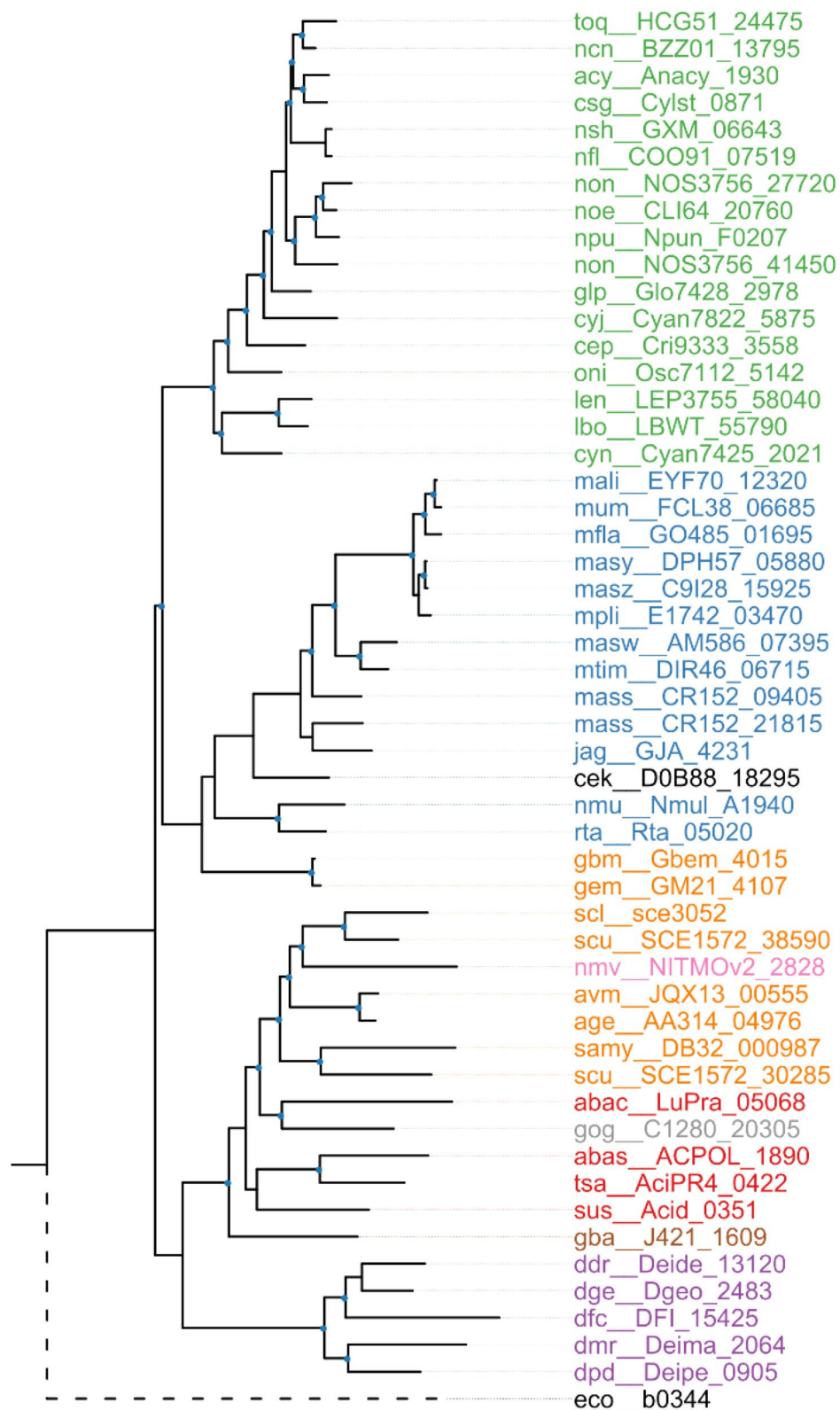


**Figure 1.** Phylogenetic analysis of Nf-LacZ (COO91\_07519) with its top 50 similar homologs from the KEGG database. The nodes with bootstrap values higher than 70% were highlighted with blue dots. The lacZ homologs from Cyanobacteria (green) form a distinct clade. The homologs from Betaproteobacteria were highlighted in blue, the homologs from Deltaproteobacteria were highlighted in orange, the homologs from Acidobacteria were highlighted in red, and the homologs from Deinococcus-Thermus group were highlighted in purple. The species names for these proteins were included in supplemental table S1.

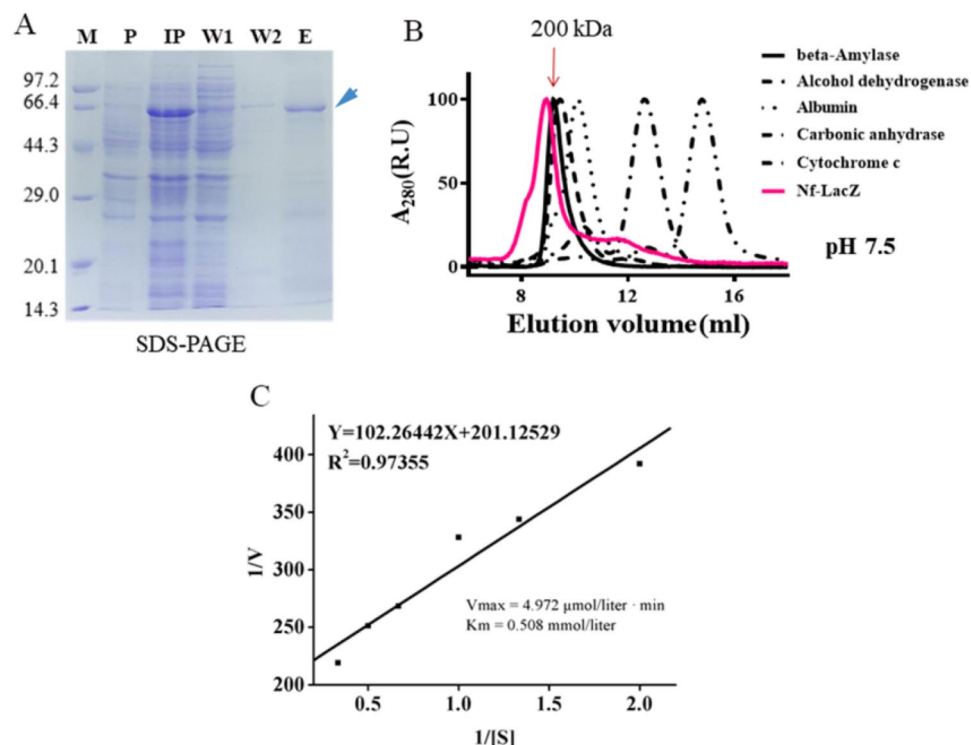


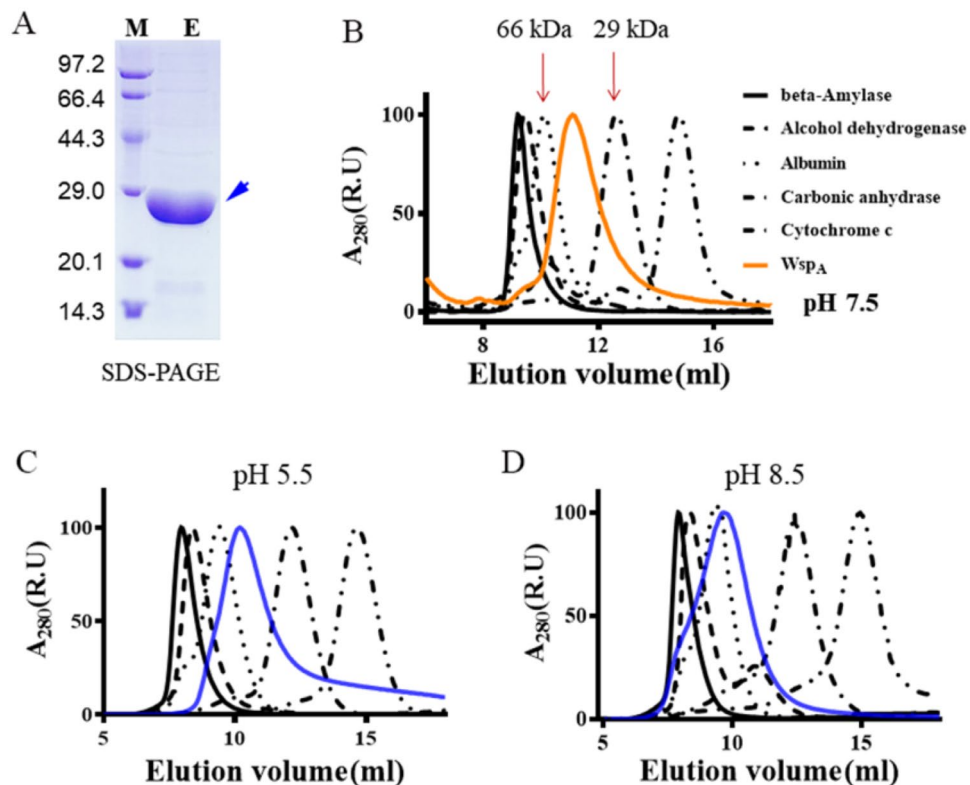
**Figure 2.** In vitro expression and enzymatic analysis of Nf-LacZ protein. (A) In vitro expression of Nf-LacZ by the *E. coli* BL21/pET28a protein expression system. M marker protein, P total proteins before IPTG induction, IP total proteins after IPTG induction, W1 and W2 washed fractions, E eluted fraction. Blue arrow points to the Nf-LacZ protein. (B) The protein polymerization state analyzed by FPLC. Molecular weight markers: beta-amylase, 200 kDa; alcohol dehydrogenase, 150 kDa; albumin, 66 kDa; carbonic anhydrase, 29 kDa; cytochrome c, 12.4 kDa. (C) Michaelis kinetic analysis.  $V_{max}$  and  $K_m$  values were calculated. ONPG serves as the substrate. Reaction was conducted at 45 °C and pH 8.0.

## Discussion

Microbial  $\beta$ -galactosidases hold particular importance due to their wide applications in food industries. They are also important tools for glycosylation of vital molecules in the medicine and cosmetic industries<sup>7</sup>. Characterization of new  $\beta$ -galactosidases from natural resources can enrich glycosidase libraries. This study conducted comparative characterization of two  $\beta$ -galactosidases Nf-LacZ and WspA1 from the terrestrial cyanobacterium *N. flagelliforme*, with more focus on the latter based on the previous research<sup>18</sup>. The LacZ homologs from some cyanobacteria form a distinct clade (Fig. 1). Biochemical analysis verified that Nf-LacZ functions as a  $\beta$ -galactosidase. However, Nf-LacZ shares only 25.2% sequence identity (Query coverage, 75%; E-value,  $4e-21$ ) with *E. coli* LacZ (JW0335). The  $K_m$  values for *E. coli* LacZ with ONPG as the substrate ranged from 0.12 to 0.82 mmol/liter at specific conditions<sup>39–41</sup>. The  $K_m$  value (0.5 mmol/liter) of Nf-LacZ falls in that range. The active form of *E. coli* LacZ is a tetramer<sup>9</sup>. According to the gel filtration assay, the size of native Nf-LacZ was larger than 200 kDa, implying that it is at least a trimer or larger. Its precise active form remains to be clarified.

By employing *E. coli* cell as a host, expression and production of recombinant proteins are not always successful and sometimes lead to form inclusion bodies<sup>42</sup>. The case is same for the full-length WspA1 protein and thus the protein truncation strategy was considered in the in vitro expression. The truncated proteins of WspA1 without the N-terminus (Fig. 5A) could be all obtained in soluble state. In most cases, we used Wsp<sub>A</sub> for biochemical characterization. As indicated by the gel filtration assay, native WspA1 should be a dimer and pH alteration cannot dissociate the dimer. Cold-active  $\beta$ -galactosidases are an attractive group identified in low temperature-adapted microorganisms<sup>10</sup>. Two cold-active  $\beta$ -galactosidases from *Paracoccus* sp. 32d and *Arthrobacter* sp. 32cB are also dimers in their native form<sup>43,44</sup>. WspA1 has no significant sequence similarity to the two enzymes. WspA1 and its homologs are found in some colonial *Nostoc* species, including *N. flagelliforme*, *N. commune*, *Nostoc sphaeroides* and *Nostoc verrucosum*<sup>18,19,45</sup>. Thus, WspA proteins may also represent a novel group of  $\beta$ -galactosidase.

Nf-LacZ and Wsp<sub>A</sub> have other different biochemical features. The optimum temperatures for the two enzymes are 40 °C and 45 °C, respectively, and both are very sensitive to higher temperature. The optimum pH values for them are 6.5 and 8.0, respectively, but Nf-LacZ seems more resistant to lower pH than Wsp<sub>A</sub><sup>18</sup> (Supplemental



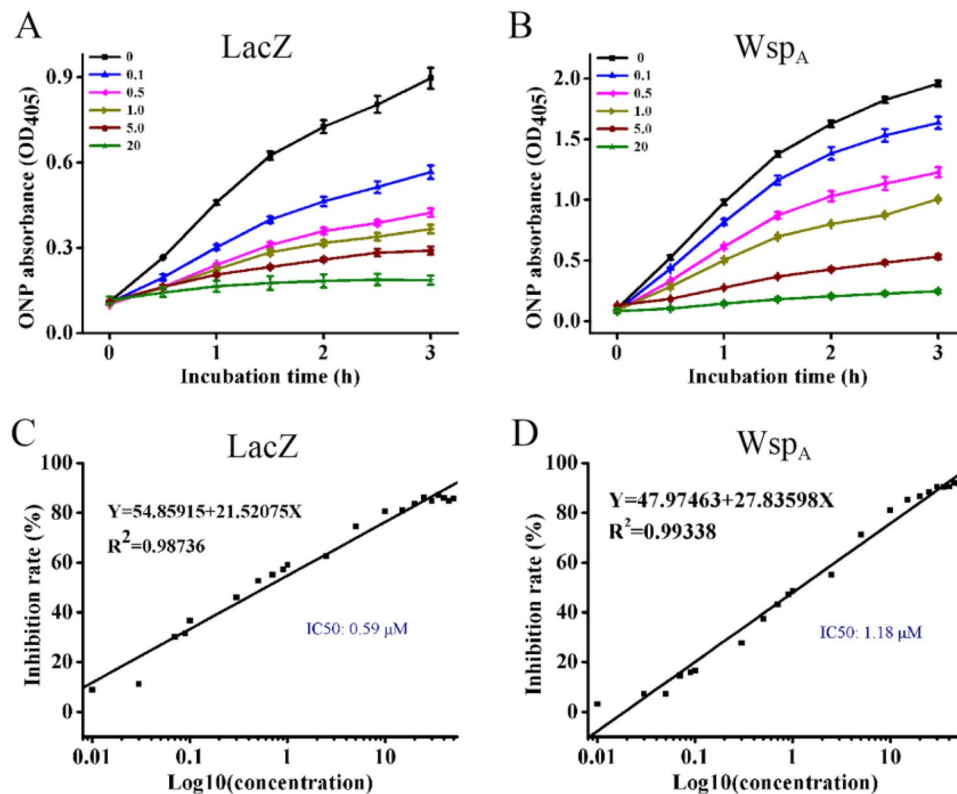
**Figure 3.** In vitro expression of Wsp<sub>A</sub> and analysis of the protein polymerization state. (A) In vitro expression of Wsp<sub>A</sub> by the *E. coli* BL21/pET28a protein expression system. M marker protein, E eluted fraction. Blue arrow points to the target protein. (B) The protein polymerization state of native Wsp<sub>A</sub> analyzed by FPLC at pH 7.5. (C) The effect of unfavorable acidic condition (pH 5.5) on the dimer of Wsp<sub>A</sub>. (D) The effect of unfavorable alkaline condition (pH 8.5) on the dimer of Wsp<sub>A</sub>.

Fig. S1). The pH value of extracellular polysaccharide matrix is around 7.6 in *N. flagelliforme*<sup>46</sup>, which may guarantee that the secreted WspA could function effectively in the matrix. In contrast, Nf-LacZ is an intracellular protein in *N. flagelliforme*, since we did not detect this protein by mass spectrometry analysis of the exoproteins. The activities of both enzymes are stimulated by Mg<sup>2+</sup>, but Ca<sup>2+</sup> is inhibitory for WspA. An in vitro experiment found that WspA could bind the UV-A/B absorbing pigment scytonemin through non-covalent interactions<sup>19</sup>. It implied that the activity of WspA might also be affected by the scytonemin molecule in the extracellular polysaccharide matrix. In addition, it was found that Nf-LacZ and WspA have similar *K<sub>m</sub>* values, but the latter is less sensitive to the inhibitor GBS.

Our previous study showed that the activity of Wsp<sub>B</sub> (Fig. 5A) was lower than that of Wsp<sub>A</sub><sup>18</sup>. A derived question is which sequence region or domain in WspA1 is critical for the activity. The truncation test of WspA1 indicated that Wsp<sub>C2</sub> (114 aa) can be recognized as the minimum central region with glycosyl hydrolytic and transgalactosylation activities. The smaller Wsp<sub>C3</sub> (94 aa) has a very weak glycosyl hydrolytic activity, which implies that it might be the primitive sequence for the evolution of WspA1. Searching Wsp<sub>C3</sub> against the NCBI nr database showed that this sequence was highly conserved (Supplemental Fig. S2). The species/strains having WspA homologs share a common feature of dense extracellular polysaccharide matrix. WspA was suggested to play a crucial role in the regulation of structural dynamics of the polysaccharide matrix for coping with periodic desiccation<sup>18</sup>. Thus, the present protein truncation analysis of WspA1 would advance our understanding on the evolution and function of WspA in those glycan-rich *Nostoc* species.

As the above mentioned, Wsp<sub>N</sub> was prone to cause the forming of inclusion bodies in the *E. coli* expression system. We had speculated that Wsp<sub>N</sub> might have a potential role in facilitating the export of WspA1 from cells. Our results showed that WspA1::GFP and Wsp<sub>N</sub>::GFP could be secreted from the cell in the form of small particles (fluorescent foci), while Wsp<sub>B</sub>::GFP could not (Fig. 6). The forming of secreted particles was also observed in our previous study in which WspA1::GFP transgenic *Arabidopsis* plants were generated<sup>22</sup>. Wsp<sub>N</sub> is not a typical signal peptide as predicted by SignalP<sup>47</sup>. Thus, Wsp<sub>N</sub> may represent a special or atypical transport way. The membrane-fusion potential of Wsp<sub>N</sub> might also be an important reason for the forming of insoluble WspA1 in the *E. coli* expression system. Longer or shorter similar sequences of Wsp<sub>N</sub> can be found in several other WspA





**Figure 4.** The inhibitory effects of GBS on the activities of Nf-LacZ and Wsp<sub>A</sub> (A,B), the galactosyl hydrolytic reactions of Nf-LacZ and Wsp<sub>A</sub> in presence of different concentrations of GBS, respectively. GBS concentration: 0 ~ 20  $\mu M$ . The absorbance of the reaction product ONP at 405 nm (OD<sub>405</sub>) was detected. Data shown are means  $\pm$  SD ( $n = 3$ ). (C,D), determination of the  $IC_{50}$  values of GBS inhibition on the activities of Nf-LacZ and Wsp<sub>A</sub>, respectively. GBS concentration ranged from 0.01  $\mu M$  to 50  $\mu M$  in the tests.

homologs, AHB33430, QFS48983, QFS48982, and WP\_100897955 (NCBI; Supplemental Fig. S2). However, it was also reported that the two WspA proteins (AUB35877 and AUB35880, NCBI) could be released from the cells of a *N. flagelliforme* culture but both proteins lack the Wsp<sub>N</sub> sequence<sup>48</sup>. Thus, Wsp<sub>N</sub>-facilitated export may be an evolving new way for protein secretion.

The secreted WspA accounts for only a very minor part of the total WspA protein in the cells of *N. flagelliforme* and *N. commune*<sup>18,19</sup>. Also, it can be released from the desiccated colonies upon rehydration. In contrast, Nf-LacZ should be still a traditional intracellular  $\beta$ -galactosidase but with low sequence similarity with the well-known *E. coli* LacZ. An illustration of the two  $\beta$ -galactosidases, LacZ and WspA, in the *N. flagelliforme* cell is shown in Fig. 7.

In conclusion, we characterized some biochemical features of the two  $\beta$ -galactosidases Nf-LacZ and WspA1 from *N. flagelliforme*. They have different enzymatic characteristics and can serve as potential biocatalysts for use in food industry. Elucidation of the central active region of WspA1 provides a valuable clue for understanding its evolution. The future resolution of their crystal structures will provide more functional information.

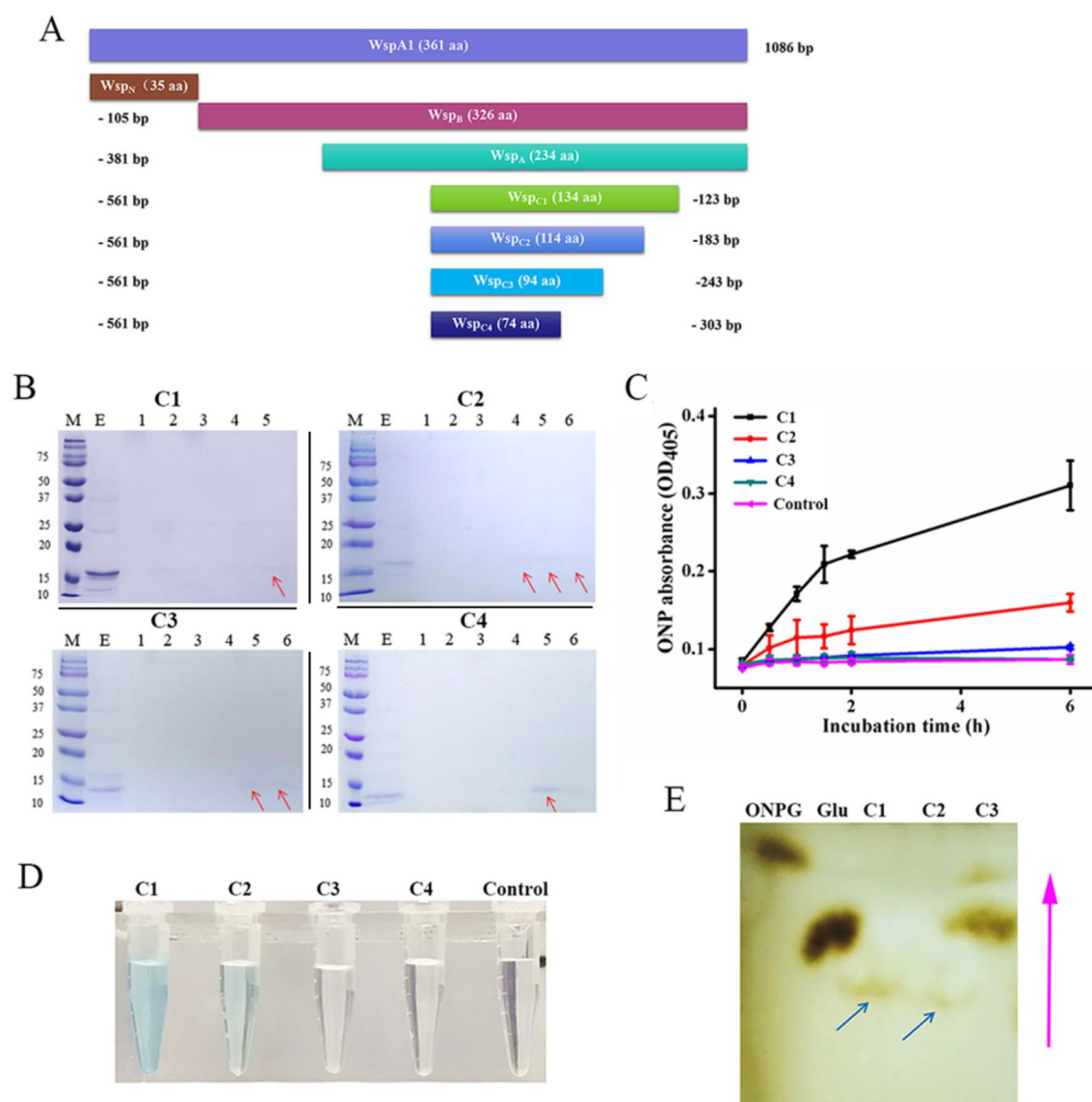


**Figure 5.** Biochemical analysis of the truncated proteins of WspA1. **(A)** An illustration of the truncated protein variants. **(B)** Protein profiles of the in vitro expressed and purified target proteins in SDS-PAGE gels. *M* marker protein, *E* eluted fraction. No. 1–6, the purified fractions by FPLC. The red arrows indicate the target proteins. C1, C2, C3 and C4 represent Wsp<sub>C1</sub>, Wsp<sub>C2</sub>, Wsp<sub>C3</sub>, and Wsp<sub>C4</sub>, respectively. **(C)** Comparative analysis of hydrolytic activities in 0.1 M PBS buffer (pH 7.5) with ONPG as the substrate. Data shown are means  $\pm$  SD ( $n=3$ ). Protein concentrations, 10  $\mu$ g/ml. ONPG, 3 mM. Control, no addition of any protein in the reaction buffer. **(D)** In vitro activity analysis of the four proteins in X-Gal buffer (pH 7.5). Similar conditions were used as in **(C)**. Reactions were performed for 6 h. **(E)** TLC analysis of the transgalactosylation activity of the truncated proteins. Glucose was used as the acceptor. Blue arrows indicate the generated products. The pink arrow indicates the solvent diffusion direction.

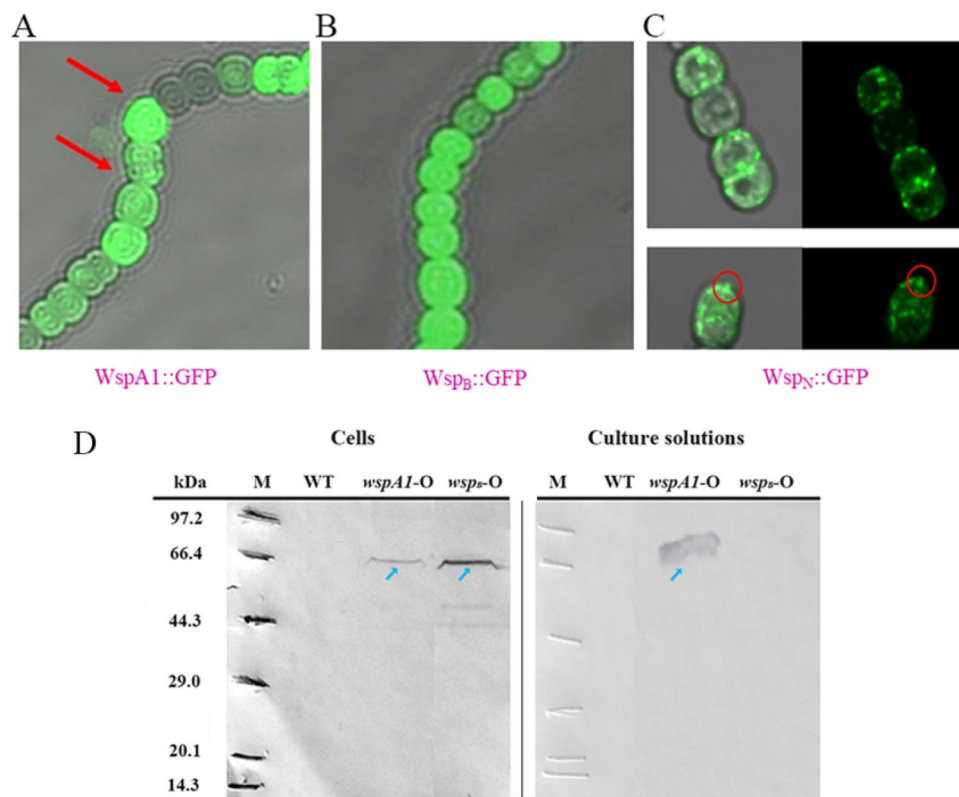


**Figure 6.** Examination of the potential export role of Wsp<sub>N</sub> in transgenic *Nostoc* sp. PCC 7120 cells. Confocal microscopy observation of the GFP-fused proteins, WspA1::GFP (A), WspB::GFP (B), and WspN::GFP (C) in transgenic cells. For panel (A,B), a 40× objective lens was used; for panel (C), a 60× objective lens was used. Red arrows point to the secreted fluorescent foci; Red circles indicate the fluorescent foci that are seemingly in the process of secretion. (D) Western blotting analysis of WspA1::GFP and WspB::GFP proteins in transgenic cells and culture solutions. An anti-WspA1 antibody was used. Blue arrows point to the target proteins. WT, wild-type cells.

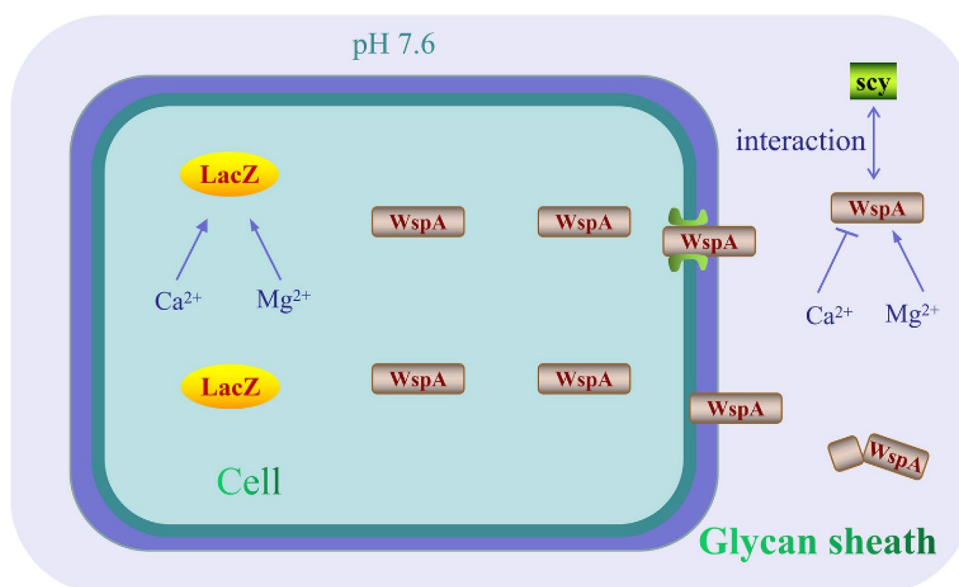


**Figure 7.** An illustration of the two  $\beta$ -galactosidases LacZ and WspA in a cell of *N. flagelliforme*. LacZ is located intracellularly. WspA is stored intracellularly, but can be secreted into the glycan sheath upon rehydration. The activities of both enzymes are promoted by Mg<sup>2+</sup>, while Ca<sup>2+</sup> is inhibitory for WspA. In the glycan sheath, the activity of WspA may also be affected by the extracellular pigment scytonemin and its own hydrolysis. scy scytonemin.

Received: 23 June 2021; Accepted: 1 September 2021

Published online: 16 September 2021

## References

1. Saqib, S., Akram, A., Halim, S. A. & Tassaduq, R. Sources of  $\beta$ -galactosidase and its applications in food industry. *3 Biotech.* **7**, 79 (2017).
2. Movahedpour, A. *et al.*  $\beta$ -Galactosidase: From its source and applications to its recombinant form. *Biotechnol. Appl. Biochem.* <https://doi.org/10.1002/bab.2137> (2021).
3. Husain, Q. Beta galactosidases and their potential applications: A review. *Crit. Rev. Biotechnol.* **30**, 41–62 (2010).
4. Benešová, E., Šučur, Z., Těšínský, M., Spiwok, V. & Lipovová, P. Transglycosylation abilities of  $\beta$ -d-galactosidases from GH family 2. *3 Biotech.* **11**, 168 (2021).
5. Cheng, W. *et al.* Effects of a galacto-oligosaccharide-rich diet on fecal microbiota and metabolite profiles in mice. *Food Funct.* **9**, 1612–1620 (2018).
6. Chandrasekar, B. & van der Hoorn, R. A. Beta galactosidases in *Arabidopsis* and tomato—a mini review. *Biochem. Soc. Trans.* **44**, 150–158 (2016).
7. Lu, L., Guo, L., Wang, K., Liu, Y. & Xiao, M.  $\beta$ -Galactosidases: A great tool for synthesizing galactose-containing carbohydrates. *Biotechnol. Adv.* **39**, 107465 (2020).
8. Bartesaghi, A., Matthies, D., Banerjee, S., Merk, A. & Subramaniam, S. Structure of  $\beta$ -galactosidase at 3.2-Å resolution obtained by cryo-electron microscopy. *Proc. Natl. Acad. Sci. USA* **111**, 11709–11714 (2014).
9. Juers, D. H., Matthews, B. W. & Huber, R. E. LacZ  $\beta$ -galactosidase: Structure and function of an enzyme of historical and molecular biological importance. *Protein Sci.* **21**, 1792–1807 (2012).
10. Mangiagalli, M. & Lotti, M. Cold-active  $\beta$ -galactosidases: Insight into cold adaption mechanisms and biotechnological exploitation. *Mar. Drugs* **19**, 43 (2021).
11. Higuchi, Y. *et al.* Identification and characterization of a novel  $\beta$ -D-galactosidase that releases pyruvylated galactose. *Sci. Rep.* **8**, 12013 (2018).
12. Carneiro, L. A. B. C., Yu, L., Dupree, P. & Ward, R. J. Characterization of a  $\beta$ -galactosidase from *Bacillus subtilis* with transgalactosylation activity. *Int. J. Biol. Macromol.* **120**, 279–287 (2018).
13. Zanette, C. M., Mariano, A. B., Yukawa, Y. S., Mendes, I. & Spier, M. R. Microalgae mixotrophic cultivation for  $\beta$ -galactosidase production. *J. Appl. Phycol.* **31**, 1597–1606 (2019).
14. Bentahar, J., Doyen, A., Beaulieu, L. & Deschênes, J. S. Investigation of  $\beta$ -galactosidase production by microalga *Tetrademus obliquus* in determined growth conditions. *J. Appl. Phycol.* **31**, 301–308 (2019).
15. Brasil, B. S. A. F., Siqueira, F. G., Salum, T. F. C., Zanette, Z. M. & Spier, M. R. Microalgae and cyanobacteria as enzyme biofactories. *Alg. Res.* **25**, 76–89 (2017).
16. Gao, K. Chinese studies on the edible blue-green alga, *Nostoc flagelliforme*: A review. *J. Appl. Phycol.* **10**, 37–49 (1998).
17. Morsy, F. M., Kuzuha, S., Takani, Y. & Sakamoto, T. Novel thermostable glycosidases in the extracellular matrix of the terrestrial cyanobacterium *Nostoc commune*. *J. Gen. Appl. Microbiol.* **54**, 243–252 (2008).
18. Liu, W., Cui, L., Xu, H., Zhu, Z. & Gao, X. Flexibility-rigidity coordination of the dense exopolysaccharide matrix in terrestrial cyanobacteria acclimated to periodic desiccation. *Appl. Environ. Microbiol.* **83**, e01619–17 (2017).
19. Wright, D. J. *et al.* UV irradiation and desiccation modulate the three-dimensional extracellular matrix of *Nostoc commune* (Cyanobacteria). *J. Biol. Chem.* **280**, 40271–40281 (2005).
20. Gao, X., Xu, H. & Yuan, X. The overlooked genetic diversity in the dryland soil surface-dwelling cyanobacterium *Nostoc flagelliforme* as revealed by the marker gene *wspA*. *Microb. Ecol.* **81**, 828–831 (2021).
21. Shang, J. L. *et al.* Genomic and transcriptomic insights into the survival of the subaerial cyanobacterium *Nostoc flagelliforme* in arid and exposed habitats. *Environ. Microbiol.* **21**, 845–863 (2019).
22. Ai, Y., Yang, Y., Qiu, B. & Gao, X. Unique WSPA protein from terrestrial macroscopic cyanobacteria can confer resistance to osmotic stress in transgenic plants. *World J. Microbiol. Biotechnol.* **30**, 2361–2369 (2014).
23. Jones, G. L. ELECTROPHORESIS | One-Dimensional Sodium Dodecyl Sulfate Polyacrylamide Gel Electrophoresis. In *Encyclopedia of Separation Science* Vol. 137 (ed. Wilson, I. D.) 1309–1315 (Academic Press, 2000).
24. Yang, Y. W. *et al.* Orange and red carotenoid proteins are involved in the adaptation of the terrestrial cyanobacterium *Nostoc flagelliforme* to desiccation. *Photosynth. Res.* **140**, 103–113 (2019).
25. Bradford, M. M. A rapid and sensitive method for the quantitation of microgram quantities of protein utilizing the principle of protein-dye binding. *Anal. Biochem.* **72**, 248–254 (1976).
26. Irvine, G. B. Determination of molecular size by size-exclusion chromatography (gel filtration). *Curr. Protoc. Cell Biol.* **5**, 5 (2001).
27. Raadsveld, C. W. & Klomp, H. Thin-layer chromatographic analysis of sugar mixtures. *J. Chromatogr. A* **57**, 99–106 (1971).
28. Georgakis, N. *et al.* Determination of half-maximal inhibitory concentration of an enzyme inhibitor. *Methods Mol. Biol.* **2089**, 41–46 (2020).
29. Dai, G., Deblois, C. P., Liu, S., Juneau, P. & Qiu, B. Differential sensitivity of five cyanobacterial strains to ammonium toxicity and its inhibitory mechanism on the photosynthesis of rice-field cyanobacterium Ge-Xian-Mi (*Nostoc*). *Aquat. Toxicol.* **89**, 113–121 (2008).
30. Zhang, L. C., Chen, Y. F., Chen, W. L. & Zhang, C. C. Existence of periplasmic barriers preventing green fluorescent protein diffusion from cell to cell in the cyanobacterium *Anabaena* sp. strain PCC 7120. *Mol. Microbiol.* **70**, 814–823 (2008).
31. Gao, X., Xu, H., Zhu, Z., She, Y. & Ye, S. Improved production of echinenone and canthaxanthin in transgenic *Nostoc* sp. PCC 7120 overexpressing a heterologous *crtO* gene from *Nostoc flagelliforme*. *Microbiol. Res.* **236**, 126455 (2020).
32. Wolk, C. P., Vonshak, A., Kehoe, P. & Elhai, J. Construction of shuttle vectors capable of conjugative transfer from *Escherichia coli* to nitrogen-fixing filamentous cyanobacteria. *Proc. Natl. Acad. Sci. USA* **81**, 1561–1565 (1984).
33. Zhao, X. M., Bi, Y. H., Chen, L., Hu, S. & Hu, Z. Y. Responses of photosynthetic activity in the drought-tolerant cyanobacterium, *Nostoc flagelliforme* to rehydration at different temperature. *J. Arid Environ.* **72**, 370–377 (2008).
34. Katoh, K., Misawa, K., Kuma, K. & Miyata, T. MAFFT: A novel method for rapid multiple sequence alignment based on fast Fourier transform. *Nucleic Acids Res.* **30**, 3059–3066 (2002).
35. Capella-Gutiérrez, S., Silla-Martínez, J. M. & Gabaldón, T. trimAl: A tool for automated alignment trimming in large-scale phylogenetic analyses. *Bioinformatics* **25**, 1972–1973 (2009).
36. Minh, B. Q. *et al.* IQ-TREE 2: New models and efficient methods for phylogenetic inference in the genomic era. *Mol. Biol. Evol.* **37**, 1530–1534 (2020).
37. Madadlou, A., O'Sullivan, S. & Sheehan, D. Fast protein liquid chromatography. *Methods Mol. Biol.* **681**, 439–447 (2011).
38. McGuffin, L. J., Bryson, K. & Jones, D. T. The PSIPRED protein structure prediction server. *Bioinformatics* **16**, 404–405 (2000).
39. Huber, R. E., Parfett, C., Woulfe-Flanagan, H. & Thompson, D. J. Interaction of divalent cations with beta-galactosidase (*Escherichia coli*). *Biochemistry* **18**, 4090–4095 (1979).
40. Roth, N. J. & Huber, R. E. The beta-galactosidase (*Escherichia coli*) reaction is partly facilitated by interactions of His-540 with the C6 hydroxyl of galactose. *J. Biol. Chem.* **271**, 14296–14301 (1996).

41. Xu, J., McRae, M. A., Harron, S., Rob, B. & Huber, R. E. A study of the relationships of interactions between Asp-201, Na<sup>+</sup> or K<sup>+</sup>, and galactosyl C6 hydroxyl and their effects on binding and reactivity of beta-galactosidase. *Biochem. Cell Biol.* **82**, 275–284 (2004).
42. Gräslund, S. *et al.* Protein production and purification. *Nat. Methods* **5**, 135–146 (2008).
43. Pawlak-Szukalska, A., Wanarska, M., Popinigis, A. T. & Kur, J. A novel cold-active  $\beta$ -D-galactosidase with transglycosylation activity from the Antarctic *Arthrobacter* sp. 32cB—Gene cloning, purification and characterization. *Proc. Biochem.* **49**, 2122–2133 (2014).
44. Wierzbicka-Woś, A. *et al.* A novel cold-active  $\beta$ -D-galactosidase from the *Paracoccus* sp. 32d—Gene cloning, purification and characterization. *Microb. Cell Fact.* **10**, 108 (2011).
45. Arima, H. *et al.* Molecular genetic and chemotaxonomic characterization of the terrestrial cyanobacterium *Nostoc commune* and its neighboring species. *FEMS Microbiol. Ecol.* **79**, 34–45 (2012).
46. Gao, X., Liu, L. T. & Liu, B. Dryland cyanobacterial exopolysaccharides show protection against acid deposition damage. *Environ. Sci. Pollut. Res.* **26**, 24300–24304 (2019).
47. Almagro Armenteros, J. J. *et al.* SignalP 5.0 improves signal peptide predictions using deep neural networks. *Nat. Biotechnol.* **37**, 420–423 (2019).
48. Yuan, X. L. *et al.* Investigations of solid culture-induced acquisition of desiccation tolerance in liquid suspension culture of *Nostoc flagelliforme*. *J. Appl. Phycol.* <https://doi.org/10.1007/s10811-021-02550-9> (2021).

## Author contributions

Data curation, L.L. and L.C.; Investigation, L.L., L.C. and X.G.; Methodology, L.L., L.C., K.L. and B.J.; Supervision, X.G. and K.L.; Validation, B.J.; Writing—draft manuscript, X.G.; Writing—review & editing, T.Z., B.J. and K.L. All authors reviewed the manuscript.

## Funding

We acknowledge the support from the National Natural Science Foundation of China (No. 31670104) and the Key Project of Natural Science of Shaanxi Province, China (No. 2020JZ-51).

## Competing interests

The authors declare no competing interests.

## Additional information

**Supplementary Information** The online version contains supplementary material available at <https://doi.org/10.1038/s41598-021-97929-6>.

**Correspondence** and requests for materials should be addressed to X.G.

**Reprints and permissions information** is available at [www.nature.com/reprints](http://www.nature.com/reprints).

**Publisher's note** Springer Nature remains neutral with regard to jurisdictional claims in published maps and institutional affiliations.



**Open Access** This article is licensed under a Creative Commons Attribution 4.0 International License, which permits use, sharing, adaptation, distribution and reproduction in any medium or format, as long as you give appropriate credit to the original author(s) and the source, provide a link to the Creative Commons licence, and indicate if changes were made. The images or other third party material in this article are included in the article's Creative Commons licence, unless indicated otherwise in a credit line to the material. If material is not included in the article's Creative Commons licence and your intended use is not permitted by statutory regulation or exceeds the permitted use, you will need to obtain permission directly from the copyright holder. To view a copy of this licence, visit <http://creativecommons.org/licenses/by/4.0/>.

© The Author(s) 2021